EFFECT OF SELECTED PARAMETERS ON FDM-HIGH-SPEED 3D PRINTED SPECIMEN PROPERTIES

JAKUB KRUZLIAK[1], LADISLAV MOROVIC[1], MAROS MARTINKOVIC[1], JANA SUGAROVA[1]

[1]Slovak University of Technology in Bratislava, Faculty of Materials Science and Technology in Trnava, Institute of Production Technologies, Trnava, Slovakia

DOI: 10.17973/MMSJ.2025_10_2025093

ladislav.morovic@stuba.sk

The paper investigates the influence of nozzle temperature (190 and 230 °C) and print speed (50, 100, 150, 200, 250 and 300 mm/s) on the tensile force of polylactic acid (PLA) and high-speed PLA (HS-PLA) test specimens fabricated via additive manufacturing method Fused Deposition Modelling (FDM). Results show that PLA test specimens printed at 230 °C exhibits tensile forces up to 2000 N, over three times higher than test specimens printed at 190 °C. Tensile force for PLA decreases between 50–100 mm/s but partially recovers near 250 mm/s. HS-PLA shows relatively consistent tensile force values across the tested print speeds and temperatures, indicating better stability compared to PLA. These findings highlight the significant effect of nozzle temperature and print speed on mechanical performance, providing useful insights for the application of FDM in HS 3D printing. As HS 3D printing gains traction, the paper emphasizes not only hardware improvements but also the critical role of material selection.

KEYWORDS

additive manufacturing, FDM, nozzle temperature, print speed, high-speed 3D printing, PLA, HS-PLA, mechanical properties, tensile force, layer adhesion

1 INTRODUCTION

In recent times, the concept of FDM HS 3D printing has gained popularity. To fully understand how HS 3D printers operate and what they ultimately offer, it is essential to first comprehend the limitations and challenges associated with HS 3D printing.

The limitations of FDM HS 3D printing generally apply to desktop 3D printers. This is because such 3D printers, due to their affordability and compact design, are more susceptible to vibrations caused by print head motion. Desktop 3D printer heads are also typically smaller than those of industrial machines, resulting in a reduced ability to handle high material flow rates through the nozzle—an essential requirement for HS 3D printing. Therefore, the maximum achievable print speed, while maintaining acceptable quality, depends on the following three factors: (1) the 3D printer's ability to suppress vibrations that deteriorate print quality, (2) the maximum material flow rate the print head can achieve, (3) the thermal properties of the printing material (which directly affect the maximum volumetric flow rate) [Filament2print 2023].

The stability of material extrusion is a critical factor in HS FDM printing, influencing both dimensional accuracy and surface quality. Geng [2019] investigated this issue using polyetheretherketone (PEEK) filament and found that the extrusion speed strongly affects melt pressure, filament diameter and surface morphology. A fluctuating extrusion force was identified as a primary factor in reducing printing stability. The study demonstrated that optimized control algorithms linking extrusion speed to extrusion diameter could enhance printing stability, thus improving both accuracy and surface finish. Although the material in question differed from PLA, the principles observed remain relevant for FDM printing with polymeric filaments at HSs.

During HS 3D printing, the print head and the nozzle extruding the build or support material operate across a wide range of speeds—from 0 mm/s up to the maximum. The higher the maximum speed, the broader the range of speeds experienced. A critical issue arises when defining nozzle temperature, which typically remains constant throughout the process. However, the temperature needed to maintain consistent extrusion changes dynamically with actual print speed. Due to this inconsistent extrusion, surface quality varies across the print, leading to a phenomenon known as shark skin, where the surface shifts from glossy to matte [Polymaker 2023b].

A review of the literature provided key insights that informed the practical section of this study. Among these is the principle of the FDM process, in which material is deposited layer-by-layer while simultaneously melting and bonding with the previously printed layer [Redwood 2017]. This layer-by-layer nature of the process is a major factor contributing to the potential for delamination in printed parts. Another important factor influencing mechanical properties is cooling of the extruded material. As Siemiński [2021] notes, greater cooling efficiency often results in weaker interlayer bonding. A crucial finding identified in the literature review was the specific definition of what qualifies as HS 3D printing, which is marked by a volumetric flow rate threshold of 24 mm^3/s [Polymaker 2023b]. This parameter defines the performance boundaries of 3D printers under HS 3D printing conditions. Another critical parameter is the layer time (see section 2.2), which significantly affects not only dimensional and geometric accuracy but also overall mechanical performance. To ensure the objectivity and reliability of this study, all these parameters were considered.

The mechanical properties of FDM printed parts—particularly tensile strength—have been shown to deteriorate with increasing printing speed. Multiple studies have confirmed this trend for PLA material. Miazio [2019] found that the maximum breaking force of PLA specimens declined significantly at print speeds above 80 mm/s, even though the strength values had stabilised in the 50–80 mm/s range. This suggests that while moderate speed increases may be tolerated, a threshold exists beyond which material performance is compromised.

Similarly, Kartal [2024] conducted a comprehensive study on PLA samples printed at speeds ranging from 15 to 105 mm/s. Their findings indicated a clear trade-off between production speed and mechanical performance. Tensile strength decreased by approximately 27%, from 60 MPa to 44 MPa, while surface roughness increased substantially. This emphasizes the need for balancing efficiency with structural integrity, particularly for functional applications.

A number of factors contribute to this phenomenon, including insufficient layer adhesion, increased porosity and incomplete melting of filament material at HS. Kamer [2022] reported that PLA samples printed at HSs exhibited lower mass, reduced hardness and increased porosity, which negatively affected overall strength. These results were consistent across two different desktop 3D printers, suggesting that the issue is inherent to the FDM process rather than machine-specific.

In contrast, recent studies have investigated HS-optimized materials, such as HS-PLA, which show promising results. Lorkowski [2025] tested HS-PLA test specimens at speeds up to

500 mm/s and found only minimal reduction in mechanical strength when the material was properly selected and orientation controlled. Furthermore, post-processing techniques such as ironing were found to enhance strength properties by reducing stress concentrations and improving layer bonding. These findings indicate that with suitable materials and printing strategies, the negative impact of increased speed on mechanical performance can be mitigated.

In summary, the reviewed studies consistently demonstrate that increasing the print speed in FDM technology tends to reduce the mechanical strength of PLA-based specimens, primarily due to weakened layer adhesion, increased porosity and insufficient thermal bonding. However, recent research also highlights the potential of HS-optimised materials such as HS-PLA, which show promising mechanical stability even at elevated print speeds, provided that material selection, part orientation and process parameters are properly controlled. These findings underline the need to further explore the combined effects of print speed, nozzle temperature and material on mechanical performance, which forms the basis of the present study.

The goal of this study was to investigate the reduction in tensile force of test specimens resulting from increasing print speeds in FDM technology. It was hypothesized that this reduction in mechanical performance occurs as a result of exceeding the printer's capability to sustain higher volumetric flow rates. As maximum print speed increases, the 3D printer must also deliver a proportionally greater amount of material through the nozzle. Consequently, print speed increases are limited by the melting capacity of the extrusion system. It is assumed that exceeding the maximum volumetric flow rate could potentially be mitigated by increasing the nozzle temperature—this was another factor explored in the study.

This study aims to contribute to the understanding of how increased nozzle temperature and print speed affect the tensile force of PLA and HS-PLA materials in FDM 3D printing. The specifics of this research lie in the systematic comparison of two temperatures (190 and 230 °C) at six speed configurations (50, 100, 150, 200, 250 and 300 mm/s) for PLA and HS-PLA. With 120 test specimens, this study offers a comprehensive dataset and a comparative perspective that helps identify material suitability for HS 3D printing applications.

2 DESIGN OF TEST SPECIMENS AND 3D PRINTING SETUP

Experiments were conducted using test specimens made of PLA and HS-PLA materials. PLA was chosen due to its widespread use in FDM additive manufacturing, while HS-PLA was selected for the purpose of comparing its mechanical performance with standard PLA and to evaluate its potential advantages.

2.1 Test specimen preparation

Siemiński [2021] describes three possible orientation scenarios for test specimens (Fig. 1): flat (XY), on edge (XZ) and upright (ZX). Siemiński [2021] also notes that printed parts exhibit significantly greater tensile strength in the XY plane (along the layers) compared to the ZX orientation (across the layers). When testing tensile specimens, fiber structure alignment in the XZ direction tends to be more favorable than in the XY direction, making parts printed in the XZ orientation somewhat more robust.

The goal in selecting the optimal orientation was to improve surface finish, enhance mechanical strength in the desired direction, reduce the amount of support material, minimize print time and maximize dimensional accuracy [Medellin-Castillo 2019].

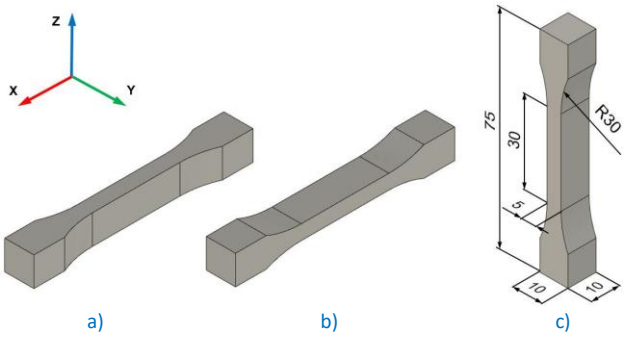

Figure 1. Possible spatial orientations of printed parts [Siemiński 2021]: a) flat (XY), b) on edge (XZ), c) upright (ZX)
The ZX orientation was used in this study, with the modified Type 1BA test specimen according to ISO 527-2, as shown in Fig. 1c.

To investigate the reduction of tensile force, a static tensile test was performed using standardized test specimens based on ISO 527-2. Although the standard Type 1BA specimen was used as a reference, the geometry was modified to suit the specifics of this study. The final specimen, shown in Fig. 1c, was used in our research. It was printed in the ZX orientation to evaluate interlayer adhesion and assess the delamination tendency of the test specimens. The thickness of test specimens was adjusted to ensure a square cross-section (10 × 10 mm) at the gripping area, providing sufficient contact with the build plate during 3D printing. Figure 1 shows the 3D model of the final test specimen designed in Autodesk Fusion 360 software.

2.2 Design and preparation of 3D printing of test specimens in Bambu Studio software

In the FDM process, where material is deposited in distinct layers, the layer time (i.e., the time taken to print each individual layer) plays a crucial role. This parameter strongly influences the cooling efficiency of the newly extruded material, which in turn can significantly impact both dimensional accuracy and the mechanical properties of the printed object. If the layer time is too short, dimensional and shape inaccuracies may occur due to material being deposited onto an insufficiently cooled previous layer.

The Bambu Studio software, used to prepare the 3D print jobs, implemented strategies to maintain optimal cooling and ensure the dimensional and shape accuracy of each layer. Although the nominal print speed was set to 300 mm/s, the software automatically slowed down the print speed throughout the height of the test specimen to maintain these quality standards. As a result, the print head was not able to reach the intended speed. The color-coded print speed distribution is shown in Fig. 2a.

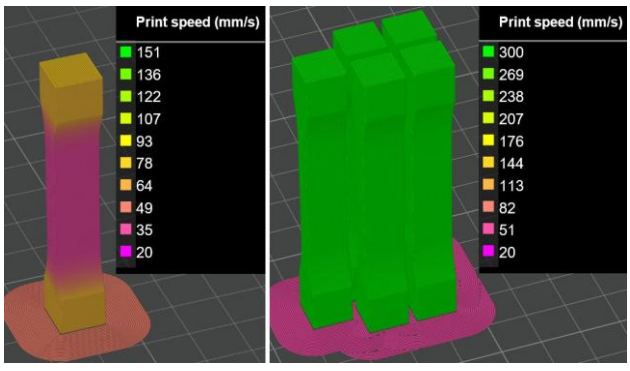

Figure 2. Visualization of: a) speed non-uniformity along the height of the test specimen, b) print speed during simultaneous printing of multiple test specimens [Kruzliak 2024]

To ensure stable 3D printing conditions, it was necessary to increase the total surface area of each layer, thereby increasing the layer time and improving cooling. To achieve this, multiple test specimens were placed on the build plate, allowing the layers of all test specimens to be printed consecutively. This approach addressed the issue of failing to reach the maximum set print speed. The configuration with multiple test specimens and the corresponding slicing strategy is in Fig. 2b.

It was essential that all test specimens—3D printed at various speeds—were produced with approximately the same layer time. The average layer time across the entire test specimen was calculated using the following formula:

$$t_v = t/n \quad (1)$$

where:

t_v – layer time (s),
t – total print time (s),
n – number of layers (-).

However, this formula only yields an average value and does not account for changes in the test specimen's dimensions along its height. Therefore, it was necessary to determine the layer time specifically within the gauge section of the test specimen, where fracture is expected to occur. This value was obtained directly from the Bambu Studio software (Fig. 3).

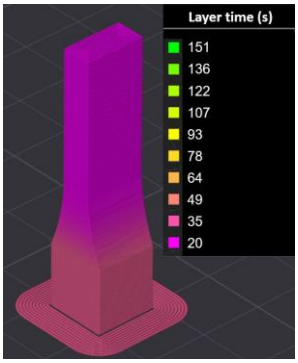

Figure 3. Illustration of the layer time parameter in the gauge section of the test specimen, where t_v = 3.1 s [Kruzliak 2024]

To ensure experimental objectivity, five test specimens were produced for each combination of print parameters, described in more detail in section 3.2. Based on previous considerations and initial trials, it was concluded that the most suitable approach was to print test specimens in batches, varying the number of parts printed simultaneously. This strategy helped minimize the influence of external factors and machine variability on the mechanical strength of the printed parts, allowing the study to focus solely on the effects of print speed and nozzle temperature. The distribution of test specimens into groups based on layer time is summarized in Tab. 1.

Group	Print speed (mm/s)	Number of specimens printed simultaneously (pcs)	Layer time (s)
1	50	2	6.2
2	100	4	7.8
3	150	5	8.2
4	200	5	7.8
5	250	5	7.6
6	300	5	7.6

Table 1. Grouping of test specimens by layer time (based on Bambu Studio) [Kruzliak 2024]

2.3 3D printing parameters of test specimens

Once the shape, dimensions and positioning of the specimens on the build plate were defined, the next step was to configure parameters in the slicing software. These determine the internal structure and cross-sectional characteristics of the printed test specimens. To meet the requirements for complete volumetric homogeneity, specimens were designed with 100% infill, 3 perimeters and 3 solid top and bottom layers (Fig. 4a).

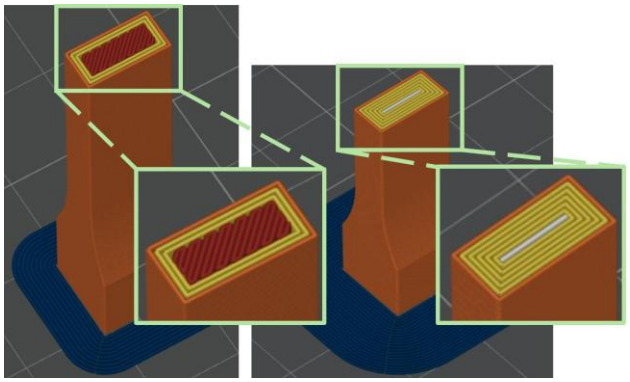

a) b)

Figure 4. Cross-sectional views of test specimens showing different internal configurations: a) standard configuration with 100% infill and 3 perimeters for volumetric homogeneity, b) modified configuration with increased number of perimeters and no solid infill (orange – outer walls, yellow – inner walls, red – solid infill, blue – brim structure for improved bed adhesion, white – gap fill) [Kruzliak 2024]

However, in the FDM process, the moving print head requires a certain travel distance to accelerate to the target print speed, and similarly, it needs to decelerate before any change in direction. If the parameters from Fig. 4a are applied, the resulting distribution of print speeds across the gauge section of the test specimen appears as shown in Fig. 5.

From the Fig. 5, it is clear that the set print speed of 300 mm/s is reached only in a small portion of the test specimen's cross-section. This is due to limited distance for the print head to accelerate and decelerate along short toolpaths. A possible solution is to increase print head acceleration to enlarge the area reaching maximum print speed. However, even with higher acceleration (within hardware limits), the improvement was minimal. The printing pattern in Fig. 6, using increased acceleration, resulted in an area printed at maximum speed that was nearly the same or only slightly larger than before.

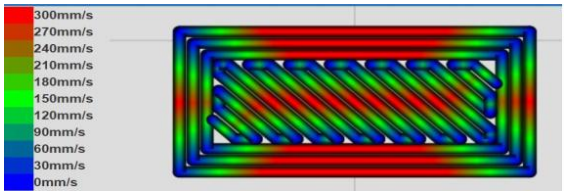

Figure 5. Color visualization of print speed distribution in a cross-section of the printed specimen at standard print head accelerations, generated with GCode Analyser [Gcodeanalyser 2020], [Kruzliak 2024]

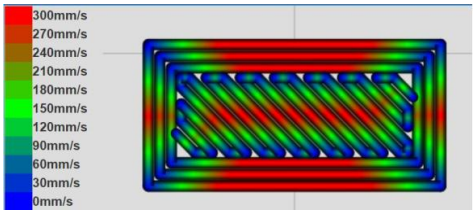

Figure 6. Color visualization of print speed distribution in a cross-section of the printed specimen at increased print head accelerations, generated with GCode Analyser [Gcodeanalyser 2020], [Kruzliak 2024]

An alternative approach was proposed: modifying the test specimen's print parameters to give the print head more time to accelerate and decelerate, and to minimize direction changes. The optimal way to extend the travel path in the gauge section was to maximize the number of perimeters and eliminate solid infill, which contains frequent direction changes. The resulting configuration is shown in Fig. 4b.

By applying this parameter setup, the area printed at maximum speed was maximized. Similar results were achieved using three perimeters combined with a fully concentric infill pattern. Other types of 100% infill patterns yielded less favorable results due to their more complex toolpaths. The configuration that produced the best performance is illustrated in Fig. 7.

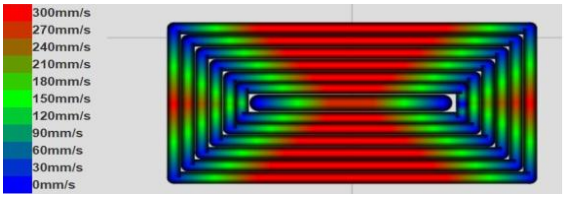

Figure 7. Print setup with six perimeters providing the largest area at maximum print speed, generated with GCode Analyser [Gcodeanalyser 2020], [Kruzliak 2024]

Another important parameter investigated in this study, which may influence the mechanical properties of the printed specimens, is the cooling fan speed. In Bambu Studio software, this parameter is defined as a percentage of the maximum fan speed. For PLA and HS-PLA, which do not experience significant shrinkage during 3D printing, the cooling fan speed was set to 100% in order to ensure dimensional and shape accuracy.

3 EXPERIMENTAL PROCEDURE

The test specimens were produced using a Bambu Lab X1C machine (Fig. 8a). This 3D printer was equipped with a textured polyetherimide (PEI) build plate, whose surface provides sufficient first-layer adhesion, helping to prevent the detachment of the printed specimens from the build surface.

The build plate temperature was set to 55 °C for both materials. The manufacturer does not recommend additional adhesives for PLA or HS-PLA to improve adhesion. However, insufficient adhesion was observed due to the small contact area, HSs, high accelerations and relatively low bed temperature, causing test specimens to detach at higher speeds.

To improve adhesion, the following adjustments were taken: (1) the build plate temperature was increased to 65 °C for the first layer and 60 °C for subsequent layers for both materials, (2) the brim width was increased to 10 mm, (3) the distance between the brim and the object was set to 0 mm, (4) a liquid adhesive agent was applied to the build plate to further support first-layer adhesion.

The 3D printer features a closed build chamber but lacks active heating. The heated bed passively warms the chamber. For this reason, chamber temperature was monitored and maintained between 34–38 °C using the circulation fan.

Before starting the production of test specimens, the device was fully lubricated, cleaned and inspected. An automatic calibration routine was initiated: (1) bed leveling (performed before each new print job), (2) micro Light Detection and Ranging (LIDAR) calibration, (3) vibration compensation calibration, (4) motor noise cancellation calibration.

Table 2 presents a comprehensive overview of the process parameters applied in the additive manufacturing of the test specimens.

Walls	Wall loops	99
	Detect thin wall	Off
Top/bottom shells	Top surface pattern	Monotonic line
	Top shell layers	4
	Top shell thickness	1.00 mm
	Top paint penetration layers	5
	Bottom surface pattern	Monotonic line
	Bottom shell layers	4
	Bottom shell thickness	0.00 mm
	Bottom paint penetration layers	3
Initial layer speed	Initial layer	50, 100, 150, 200, 250, 300 mm/s
	Initial layer infill	50, 100, 150, 200, 250, 300 mm/s
Other layers speed	Outer wall	50, 100, 150, 200, 250, 300 mm/s
	Inner wall	50, 100, 150, 200, 250, 300 mm/s
	Small perimeters	50%
	Small perimeter threshold	0
	Sparse infill	50, 100, 150, 200, 250, 300 mm/s
	Internal solid infill	50, 100, 150, 200, 250, 300 mm/s
	Vertical shell speed	80%
	Top surface	50, 100, 150, 200, 250, 300 mm/s
Travel speed	Travel	500 mm/s
Acceleration	Normal printing	10000 mm/s^2
	Travel	10000 mm/s^2
	Initial layer travel	6000 mm/s^2
	Initial layer	500 mm/s^2
	Outer wall	5000 mm/s^2
	Inner wall	0 mm/s^2
	Top surface	2000 mm/s^2
	Sparse infill	100%
Layer height	Layer height	0.20 mm
	Initial layer height	0.20 mm
Line width	Default	0.42 mm
	Initial layer	0.50 mm
	Outer wall	0.42 mm
	Inner wall	0.45 mm
	Top surface	0.42 mm
	Sparse infill	0.45 mm
	Internal solid infill	0.42 mm
	Support	0.42 mm
Temperature	Nozzle temperature	190, 230 °C

Table 2. Process parameters for additive manufacturing of test specimens

a)

b)

c)

Figure 8. Equipment and test setup: a) 3D printer Bambu Lab X1C [Bambu Lab 2023], b) test specimen clamped in the jaws of the universal testing machine [Kruzliak 2024], c) test specimen after static tensile testing [Kruzliak 2024]

3.1 Material preparation before 3D printing

Two materials from the same manufacturer were selected for testing to ensure objectivity and comparability. The selected materials were: PolyLite™ PLA as a representative of standard PLA filament without modified properties for HS applications, and PolySonic™ PLA Pro as a representative of HS-PLA, specifically engineered and optimized for such HS applications (Tab. 3).

Parameter	Testing method	PolyLite™ PLA	PolySonic™ PLA Pro
Young's modulus (XY)	ISO 527, GB/T 1040	3426.9±64.8 MPa	2360.0±30.1 MPa
Young's modulus (ZX)		3064.9±83.4 MPa	2283.3±32.1 MPa
Tensile strength (XY)	ISO 527, GB/T 1040	52.3±0.3 MPa	41.2±0.6 MPa
Tensile strength (ZX)		40.5±0.5 MPa	33.6±0.5 MPa
Elongation at break (XY)	ISO 527, GB/T 1040	6.3±0.6 %	23.4±6.3 %
Elongation at break (ZX)		1.8±0.1 %	4.9±1.1 %
Nozzle temperature	-	190–230 °C	190–210 °C
Build plate temperature	-	25–60 °C	210–230 °C
Print speed	-	40–60 mm/s	30–60 mm/s
High-speed print rate	-	-	100–300 mm/s

Table 3. Technical specifications of PolyLite™ PLA (i.e. PLA) [Polymaker 2023a] and PolySonic™ PLA Pro (i.e. HS-PLA) materials [Polymaker 2023b]

When evaluating the mechanical properties of FDM-fabricated test specimens, an important factor—alongside the type of material used—is its moisture content. High moisture levels can negatively affect the final strength and overall quality of test specimens, especially for highly hygroscopic materials. Therefore, the filaments were carefully dried in a filament drying device at 45 °C for six hours prior to printing. As a result, the moisture content of the materials during 3D printing did not exceed 30%, helping to ensure consistent mechanical performance and reproducibility of the test results.

3.2 Configuration of 3D printing parameters

After determining the maximum volumetric flow rate achievable with the specific 3D printer, parameter configurations were established for the production of the test specimens. Since nozzle temperature is the most influential factor affecting the maximum material flow rate, two temperature settings were used for each print speed:

- The lower nozzle temperature (i.e. 190 °C) was based on the bottom limit of the manufacturer's recommended range.
- The higher nozzle temperature (i.e. 230 °C) corresponded to the upper limit.

A total of 12 print configurations were tested, created by combining two nozzle temperatures (190 °C and 230 °C) with six print speeds (50, 100, 150, 200, 250, and 300 mm/s), as detailed in Tab. 4. For each material (PLA and HS-PLA), five identical test specimens were printed per configuration to ensure repeatability and statistical relevance. This resulted in 60 test specimens per material and 120 test specimens in total, enabling a structured evaluation of the combined influence of nozzle temperature and print speed on tensile force.

Table 4 presents the parameter configurations used for both PLA and HS-PLA materials. The test specimens were fabricated using identical configurations to allow for direct comparison.

Configuration	Print speed (mm/s)	Nozzle temperature (°C)	Material	No. of specimens (pcs)
C1	50	190	PLA / HS-PLA	5
C2	50	230	PLA / HS-PLA	5
C3	100	190	PLA / HS-PLA	5
C4	100	230	PLA / HS-PLA	5
C5	150	190	PLA / HS-PLA	5
C6	150	230	PLA / HS-PLA	5
C7	200	190	PLA / HS-PLA	5
C8	200	230	PLA / HS-PLA	5
C9	250	190	PLA / HS-PLA	5
C10	250	230	PLA / HS-PLA	5
C11	300	190	PLA / HS-PLA	5
C12	300	230	PLA / HS-PLA	5

Table 4. Parameter configurations for PLA and HS-PLA materials [Kruzliak 2024]

All fabricated test specimens were tested in a static tensile test using a Tinius Olsen ST300 universal testing machine, capable of applying a maximum force of 300 kN [Tinius Olsen 2024]. Mechanical grips were used to mount the specimens (Fig. 8b), and a specimen after tensile testing is shown in Fig. 8c.

In this study, tensile test results are presented as tensile force versus displacement, rather than the more commonly used tensile stress–strain curves. While stress–strain diagrams are the standard for tensile testing, particularly when an extensometer is used, our tests were conducted without one.

Without an extensometer, displacement measured at the machine's moving crosshead may be influenced by system compliance and grip-related effects. While these are expected to be minimal due to the relatively low forces applied, they can still introduce some uncertainty in calculated strain values. Therefore, the force–displacement curve provides a more reliable and direct representation of the mechanical response during testing. While stress–strain curves remain the standard

when direct strain measurement is available, force–displacement data is a suitable and widely accepted alternative under these specific testing conditions.

4 ANALYSIS AND EVALUATION OF THE IMPACT OF 3D PRINTING PARAMETERS ON TENSILE FORCE

The evaluation criterion was the maximum force reached during the static tensile test. The results were assessed separately for each material, followed by a comparison between the two materials.

4.1 PolyLite™ PLA material

The PLA material was tested in 12 different printing configurations, as shown in Tab. 4.

4.1.1 Results for PLA test specimens printed at 190 °C

This section presents the evaluation of the static tensile test results for PLA test specimens printed using configurations 1, 3, 5, 7, 9 and 11. For each configuration, 5 test specimens were tested. The individual results, as well as the mean values and standard deviations (SD) for each configuration, are listed in Tab. 5. Specimens labeled N/F (Not Functional) were excluded due to clamping failure.

Speci-men	Tensile force (N)					
	C1	C3	C5	C7	C9	C11
1	725	664	405	465	500	276
2	1060	N/F	417	N/F	452	444
3	878	333	488	438	569	236
4	916	598	459	504	452	442
5	947	609	523	392	387	445
Mean ±SD	905.2 ±121.5	551.0 ±148.2	458.4 ±49.0	449.8 ±47.1	472.0 ±67.5	368.6 ±103.8

Table 5. Results for PLA test specimens printed at a nozzle temperature of 190 °C [Kruzliak 2024]

By comparing the results across these configurations, a significant decrease in tensile force can be observed as the print speed increases.

On average, test specimens from configuration 11 exhibited nearly a 2.5-fold decrease in tensile force compared to configuration 1.

Figure 9 illustrates a typical example force–displacement curve from the tensile test for a test specimen printed at print speed of 50 mm/s and nozzle temperature of 190 °C.

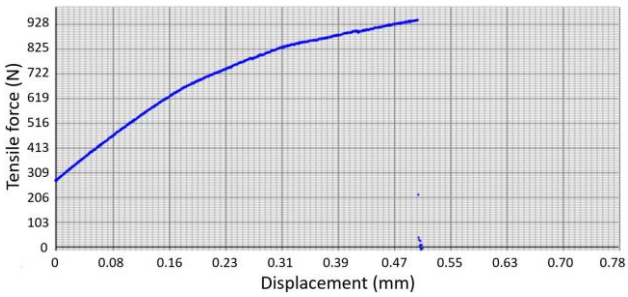

Figure 9. An example of tensile force vs. crosshead displacement curve for PLA test specimen printed at 50 mm/s print speed and 190 °C nozzle temperature [Kruzliak 2024]

The graph also reveals an initial preload force, introduced during the clamping of the test specimen in the universal testing machine's jaws. This preload was present in all tested specimens and must be taken into account; otherwise, it could lead to inaccurate or misleading results.

4.1.2 Results for PLA test specimens printed a 230 °C

This section presents the results of the static tensile tests for PLA test specimens printed using even-numbered configurations, specifically configurations: 2, 4, 6, 8, 10 and 12. The test outcomes and corresponding mean values with SD are presented in Tab. 6.

Speci-men	Tensile force (N)					
	C2	C4	C6	C8	C10	C12
1	N/F	1830	1810	1760	1840	1700
2	N/F	1870	1780	1830	1820	1670
3	1740	1790	1780	1790	1860	1730
4	1760	1790	1750	1740	1900	1750
5	1750	1760	1750	1770	1780	1740
Mean ±SD	1750.0 ±10.0	1808.0 ±42.7	1774.0 ±25.1	1778.0 ±34.2	1840.0 ±44.7	1718.0 ±32.7

Table 6. Results for PLA test specimens printed at a nozzle temperature of 230 °C [Kruzliak 2024]

In contrast to the 190 °C group, the 230 °C configurations did not show significant variation in tensile force with increasing print speed. This may be due to the higher nozzle temperature, which improves extruder melting capacity, increases volumetric flow, and enhances the material's ability to fill inter-layer gaps. These findings suggest that, under the given conditions, the tested PLA can tolerate print speeds above 300 mm/s, despite visible defects appearing at 150 mm/s in maximum volumetric flow tests.

However, evaluating tensile force above 300 mm/s properly requires modifying the test specimen design:

- The gauge section would need to have a larger cross-sectional area to ensure sufficient travel distance for the print head to reach the target speed.

- The gripping section, which contacts the print bed, would also require a larger surface area to ensure adequate first-layer adhesion.

Thus, these configurations warrant further investigation using alternative test specimen geometries.

Interestingly, a sudden drop in force was observed in all test specimens in this group during testing, often accompanied by an audible crack. This suggests that layer separation may have occurred between regions extruded at maximum print speed and those printed at reduced speed due to the acceleration/deceleration of the print head (see section 2.3). Despite partial failure, these sections often remained attached, allowing the test specimen to withstand additional loading.

The example of force–displacement curve of a test specimen printed at print speed of 50 mm/s and nozzle temperature of 230 °C is shown in Fig. 10.

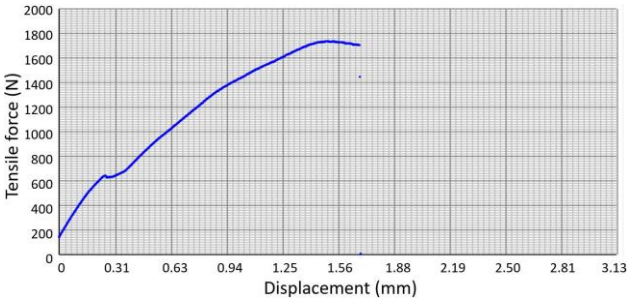

Figure 10. An example of tensile force vs. crosshead displacement curve for PLA test specimen printed at 50 mm/s print speed and 230 °C nozzle temperature [Kruzliak 2024]

The fracture surface of the same test specimen, whose force–displacement curve is displayed in Fig. 10, is shown in Fig. 11.

Figure 11. Fracture surface of the test specimen printed at print speed of 50 mm/s and nozzle temperature of 230 °C [Kruzliak 2024]

On the fracture surface, failure regions oriented perpendicular to the layer orientation, rather than along the layer lines, can be observed. This may indicate that inter-layer adhesion in this particular test specimen was stronger than the material's bulk strength, or it could be due to internal print defects, which were regularly observed in this configuration—or a combination of both. In any case, this fracture mode is preferable to inter-layer delamination, as it implies better bonding between layers.

Due to the force drop and partial fracture, these test specimens were considered non-compliant, and the most critical value to report was the force at the onset of the drop. However, the force reduction occurred irregularly across all test specimens, even among those printed with identical settings, showing no consistent pattern that could be used for analysis. Therefore, the maximum force at failure was used as the reference value, and further testing is recommended with test specimens having larger gauge cross-sections to reduce the relative impact of acceleration and deceleration phases and to maximize the region exposed to the nominal print speed.

4.2 PolySonic™ PLA Pro material

The next tested material was HS-PLA. This material was also evaluated using 12 different configurations, as shown in Tab. 4.

4.2.1 Results for HS-PLA test specimens printed at 190 °C

This section evaluates the tensile test results for HS-PLA specimens printed using configurations 1, 3, 5, 7, 9 and 11. Table 7 displays the measured values for each configuration, along with their mean values and SDs.

Speci-men	Tensile force (N)					
	C1	C3	C5	C7	C9	C11
1	943	820	789	705	640	668
2	904	N/F	779	697	663	684
3	967	816	782	732	691	659
4	970	850	669	717	729	681
5	N/F	804	789	751	678	648
Mean ±SD	946.0 ±30.5	822.5 ±19.6	761.6 ±51.9	720.4 ±21.6	680.2 ±33.2	668.0 ±15.0

Table 7. Results for HS-PLA test specimens printed at a nozzle temperature of 190 °C [Kruzliak 2024]

From Tab. 7, a gradual decrease in tensile force with increasing configuration number (i.e., with increasing print speed) can be observed. This decrease is clear, consistent, and shows no significant fluctuations, which indicates well-chosen parameters and properly controlled experimental variables. These results support the hypothesis that increasing print speed leads to a decline in mechanical properties, as the 3D printing system reaches its limit in volumetric flow rate through the nozzle.

Figure 12 presents the example of force–displacement graph for a test specimen printed at a speed of 50 mm/s and a nozzle temperature of 190 °C.

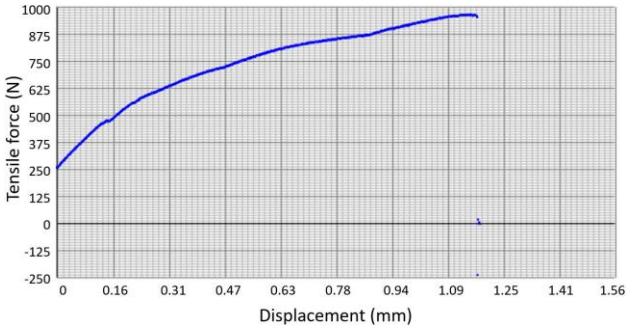

Figure 12. An example of tensile force vs. crosshead displacement curve for HS-PLA test specimen printed at 50 mm/s print speed and 190 °C nozzle temperature [Kruzliak 2024]

It can be determined from this graph that the test specimen fractured at a maximum force of approximately 900 N. The curve also demonstrates a steady increase in tensile force throughout the test, with no significant drops.

For a test specimen printed at a print speed of 250 mm/s, the force–displacement curve is very similar to the one observed at 50 mm/s. However, the maximum breaking force is reduced to 729 N, representing a decrease of approximately 20%. The example of force–displacement behavior of the test specimen printed at 250 mm/s is shown in Fig. 13.

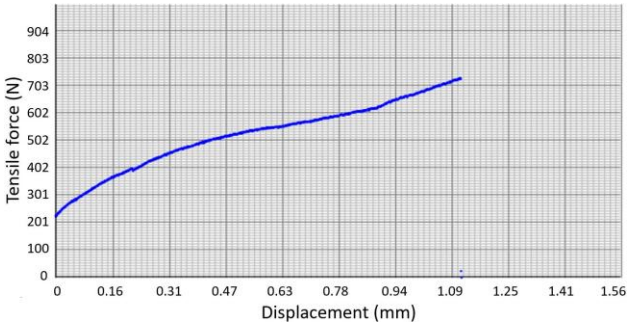

Figure 13. An example of tensile force vs. crosshead displacement curve for HS-PLA test specimen printed at 250 mm/s print speed and 190 °C nozzle temperature [Kruzliak 2024]

4.2.2 Results for HS-PLA test specimens printed at 230 °C

In this section, the results of the tensile tests for HS-PLA test specimens printed at a nozzle temperature of 230 °C were evaluated. These are the even-numbered configurations: 2, 4, 6, 8, 10, 12. Table 8 displays the test results along with their mean values and SDs.

Speci-men	Tensile force (N)					
	C2	C4	C6	C8	C10	C12
1	1040	1070	1110	1120	1110	1100
2	1000	1050	1120	1110	1090	1110
3	1010	1030	1040	1090	1100	1120
4	1010	1060	1090	1050	1090	1110
5	1010	1070	1100	1110	1130	1110
Mean ±SD	1014.0 ±15.2	1052.5 ±16.7	1092.0 ±31.1	1096.0 ±27.9	1104.0 ±16.7	1110.0 ±7.1

Table 8. Results for HS-PLA test specimens printed at a nozzle temperature of 230 °C [Kruzliak 2024]

For the test specimens tested at nozzle temperature of 230 °C, there were no significant differences observed in the maximum

tensile force, which supports the assumption that HS-PLA material has optimized properties for HS 3D printing. It appears that for test specimens printed at a nozzle temperature of 230 °C, the threshold for the decline in tensile force begins only at higher print speeds.

An interesting finding was that all test specimens in this group exhibited a desirable ductile fracture behavior. In such fractures, after reaching a certain force threshold, the force stops increasing, remains constant, or slightly decreases for a while before the final failure occurs. The example of force–displacement curve for a test specimen printed at a speed of 250 mm/s is in Fig. 14.

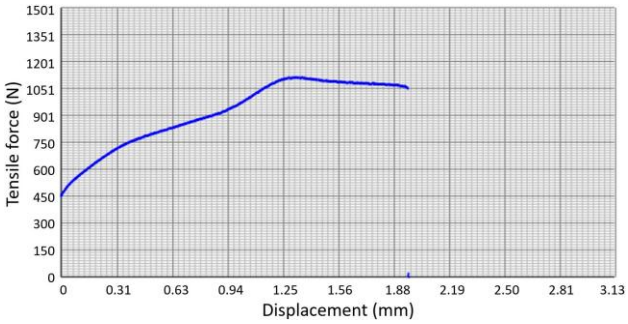

Figure 14. Ductile fracture behavior: an example of tensile force vs. crosshead displacement curve for HS-PLA test specimen printed at 250 mm/s print speed and 230 °C nozzle temperature [Kruzliak 2024]

From Fig. 14, it is evident that at a tensile force of approximately 1100 N, the increase in force halted and began to slightly decline, reaching around 1060 N at which point the specimen fully fractured. This type of failure is desirable in practice because it allows for high predictability of part behavior and enables more accurate load planning.

5 DISCUSSION

This section provides a discussion and interpretation of the experimental results obtained from tensile testing of PLA and HS-PLA test specimens. The analysis focuses on how different nozzle temperatures and print speeds influenced the tensile force of the printed test specimens.

In the graphical dependencies shown in Fig. 15, the obtained results are visualized using individual data points, while the connecting curve is only indicative. The progression between points and across groups is estimated and serves an informative purpose; it does not necessarily reflect the material's exact behavior at print speeds not tested in this study. To accurately define the trend of tensile force as a function of print speed for a specific group, additional configurations would be needed to create a denser data set and enable proper curve fitting. Further testing with more test specimens and finer print speed intervals would be required to determine the actual trend.

5.1 Discussion of results for PLA test specimens printed at 190 °C and 230 °C

This section focuses on the comparison of the results obtained from test specimens printed at nozzle temperatures of 190 °C and 230 °C. The Fig. 15 presents a graphical representation of the decrease in tensile force in relation to print speed.

The graphical dependency in Fig. 15 reveals a clear drop in tensile force within the 50–100 mm/s print speed range. Between 100–250 mm/s, the decline becomes less pronounced, and as the print speed approaches 250 mm/s, a slight increase in tensile force is observed, with a local minimum occurring around 150–200 mm/s. Beyond 250 mm/s, tensile force decreases once again, indicating a potential continued downward trend at speeds exceeding 300 mm/s.

For the test specimens printed at 230 °C, the graphical dependency looks markedly different, though some similarities with the 190 °C group are evident. Figure 15 shows the tensile force–print speed dependency for the test specimens manufactured at a nozzle temperature of 230 °C.

In the 50–100 mm/s print speed range, the trend is reversed compared to the 190 °C group. Initially, tensile force increases, then begins to decrease after reaching 100 mm/s, reaching a local minimum around 150 mm/s, a value very similar to that of the first group. Between 200–250 mm/s, tensile force starts to increase again, a trend that was also observed in the 190 °C group. After prints speed of 250 mm/s, the tensile force drops again, echoing the trend seen previously.

These similarities in the tensile force–printing speed dependencies at both 190 °C and 230 °C could be partially attributed to variations in layer time, which is defined for different print speeds in Tab. 1. From this, it can be inferred that shorter layer times result in higher tensile force, potentially due to less air exposure from the cooling system interacting with the freshly printed material. Weaker cooling efficiency could lead to greater inter-layer adhesion. However, this assumption did not hold true in all cases, and therefore requires further investigation in the following sections.

It's also important to note that slight deviations in layer time under the given experimental conditions could not be entirely eliminated. A common characteristic of both material groups is the renewed decrease in tensile force at print speeds above 250 mm/s, despite the shorter layer time at 300 mm/s compared to 250 mm/s. This suggests that, in this range, the decline in mechanical properties due to increased print speed becomes more prominent.

Even at first glance, Fig. 15 shows that the mean tensile force of test specimens printed at 230 °C is more than three times higher than that of those printed at 190 °C. This is a result of the inherent nature of the FDM process, where a newly deposited layer partially remelts the previous one. Therefore, the higher the extrusion temperature, the greater the inter-layer fusion, leading to improved adhesion.

Moreover, test specimens printed at 190 °C displayed larger SD, which are represented by the error bars in the graph (Fig. 15). In practice, this means that the mechanical properties were less consistent, suggesting a higher incidence of internal defects, which can act as stress concentrators.

Finally, a very similar trend in tensile force dependency was observed for both material groups within the 100–300 mm/s print speed range. This similarity was further analyzed in the previous part of this section.

5.2 Discussion of results for HS-PLA test specimens printed at 190 °C and 230 °C

This section presents a comparison of HS-PLA test specimens printed at nozzle temperatures of 190 °C and 230 °C. Figure 15 illustrates the dependence of tensile force on print speed for test specimens produced at 190 °C.

The evaluation of individual configurations yields data points that provide an approximate indication of the overall trend. The pattern exhibits a rapid decrease in tensile force at lower print speeds, which gradually becomes less pronounced as the speed increases. It is assumed that at print speeds above 300 mm/s, the reduction in tensile force would be even less pronounced for this type of test specimen. This assumption is based on the limited ability of the print head to reach the maximum set print speed within the gauge section's cross-sectional area.

Consequently, for test specimens with a larger cross-sectional area, the decrease in tensile force at higher print speeds may be more pronounced. However, this hypothesis requires further investigation.

Figure 15 illustrates the tensile force dependence on print speed using data points for test specimens printed at 230 °C.

Interestingly, the trend here is completely opposite to that observed in the test specimens printed at 190 °C. While the previous group showed a decrease in tensile force with increasing print speed, this group instead exhibits a slight increase in tensile force as the print speed increases. However, this increase is not significant enough to confidently identify it as a general trend. The increase in tensile force at a print speed of 300 mm/s compared to 50 mm/s is approximately 9%, suggesting that HS-PLA maintains nearly the same tensile force across the 50–300 mm/s print speed range, making it well-suited for high-speed 3D printing applications.

Figure 15 presents a summary graph showing tensile force as a function of print speed for HS-PLA at both nozzle temperatures, with error bars representing SD.

From this figure, only a slight increase in the average tensile force can be observed for test specimens printed at 230 °C compared to those printed at 190 °C. Although an increase was recorded, it was not considered as pronounced as in the case of PLA, described in section 5.1.

Different trends in the curves can also be noticed: test specimens printed at 190 °C are shown to have a decreasing tendency, whereas those printed at 230 °C are shown to exhibit an increasing or nearly constant trend. These characteristics are likely to be material-dependent and not primarily related to the parameters used in this experiment.

5.3 Comparison and discussion of PLA vs. HS-PLA performance

This section discusses the differences between PLA and HS-PLA materials. All parameters potentially influencing the final mechanical properties were kept consistent for both materials. Both materials were dried using the same drying device, under identical conditions (temperature, time and humidity), and the temperature inside the print chamber remained constant during all 3D print jobs. Figure 15 provides a comprehensive overview of the results for all configurations of both materials.

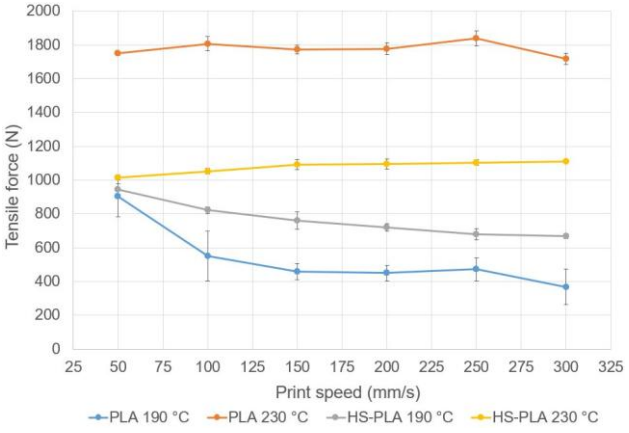

Figure 15. Comparison of tensile force dependence on print speed for PLA and HS-PLA materials [Kruzliak 2024]

This figure reveals significant differences between the two materials. PLA at a higher nozzle temperature undoubtedly delivers the highest average tensile force, while at the lower temperature, it exhibits the lowest. This suggests that PLA is not well-suited for high-speed (HS) 3D printing, as it has a limited ability to compensate for the thermal fluctuations that occur during HS printing.

On the other hand, HS-PLA appears to manage these fluctuations much more effectively, resulting in a smaller difference in average tensile force between specimens printed at 190 °C and 230 °C. It is also clear that HS-PLA cannot achieve tensile forces close to 2000 N, as observed with PLA at 230 °C.

Considering the tensile force behavior of HS-PLA at both nozzle temperatures, it can be concluded that the increase in tensile force at a print speed of 250 mm/s, observed with PLA (discussed in section 5.1), was specific to PLA and was not caused by the layer time parameter. It is likely that the differences in layer time were too small for a meaningful effect on tensile force to be produced.

5.4 Comparison with previous studies and technical explanation

The experimental results demonstrating the significant influence of nozzle temperature and print speed on the tensile force of PLA and HS-PLA test specimens align well with findings reported in the existing literature. Higher nozzle temperature (230 °C) notably improved the mechanical performance of PLA test specimens, which is consistent with the theory that increased temperature enhances interlayer bonding in the FDM process [Redwood 2017], [Siemiński 2021]. This improvement is attributed to partial remelting of the previously deposited layer during the deposition of the new layer, resulting in better adhesion and reduced internal defects [Kartal 2024].

Conversely, the observed decrease in tensile force with increasing print speed—mainly between 50 and 100 mm/s—can be explained by the technical limitations of the extruder, which at higher speeds may fail to supply material with sufficient precision. This leads to insufficient interlayer bonding and the formation of microscopic voids and cracks [Geng 2019], [Kamer 2022]. Similar effects were documented by Lorkowski [2025] and Miazio [2019], who reported deterioration of polymer mechanical properties at elevated print speeds.

Interestingly, HS-PLA exhibits more stable mechanical properties across the entire print speed range and shows less sensitivity to temperature variations, suggesting better material adaptability for HS printing [Polymaker 2023b]. This observation supports claims regarding the specialized composition of HS-PLA filaments, which provide improved flow characteristics and faster solidification without compromising interlayer adhesion [Filament2print, 2023].

The weaker mechanical properties of test specimens printed at the lower temperature (190 °C) may also result from faster cooling rates of layers, leading to inadequate bonding and increased porosity [Medellin-Castillo 2019]. This phenomenon is well documented in previous studies emphasizing that optimal printing temperature is critical for achieving desired mechanical performance [Redwood 2017].

Overall, these findings confirm that an appropriate combination of nozzle temperature and print speed is essential to maximize the strength of FDM-printed parts, corroborating the existing knowledge in additive manufacturing.

6 CONCLUSIONS

FDM is a widely used 3D printing method, offering semi-automated machines and accessible technical-grade materials. However, challenges remain—especially in HS 3D printing, where mechanical properties may deteriorate.

In the theoretical part of this thesis, the fundamental principles of the FDM method and the trend of increasing print speed

were explored. It was found that higher print speeds offer several advantages, such as shorter production times and improved process efficiency. However, potential risks were also identified—primarily the deterioration of mechanical properties as print speed increases.

The research showed that high print speeds can lead to reduced tensile force, as well as issues with dimensional accuracy and surface quality. These phenomena could impact the usability of printed parts, especially in industries requiring high mechanical durability.

In conclusion, further research and development in FDM technology are needed to reduce or eliminate mechanical performance loss at HSs. Innovations in material science, process optimization and advanced solutions could help maintain print quality while increasing speed. Further testing with various materials and parameters is essential to better understand how print speed affects mechanical properties.

Despite current limitations, the FDM printing method is continuously evolving. Research into the decline of mechanical performance caused by increased print speed is just one of many important areas requiring further attention and advancement. With ongoing development, it is possible to overcome current challenges and make FDM more reliable across a broader range of applications, with greater confidence in the strength and quality of printed components.

ACKNOWLEDGMENTS

The authors express their thanks for the financial contribution, that supports this research, namely the KEGA project 026STU-4/2023.

REFERENCES

[Bambu Lab 2023] Bambu Lab X1 Series | Desktop 3D Printer | X1-Carbon - Bambu Lab. 2025 [online] [16.04.2025]. Available form <https:// https://bambulab.com/en-eu/x1/>

[Filament2print 2023] High-speed 3D printing. 2023 [online]. 02.05.2023 [16.04.2025]. Available form <https://filament2print.com/gb/blog/184_high-speed-3d-printing.html>

[Gcodeanalyser 2020] G-Code Analyser - Analyse your 3D printing G-Code to provide accurate information such as print time and average speed. 2020 [online] [16.04.2025]. Available form <https:// www.gcodeanalyser.com/>

[Geng 2019] Geng, P., et al. Effects of extrusion speed and printing speed on the 3D printing stability of extruded PEEK filament. Journal of Manufacturing Processes, January 2016, Vol.37, pp 266-273. ISSN 1526-6125. https://doi.org/10.1016/j.jmapro.2018.11.023

[Kamer 2022] Kamer, M. S., et al. Effect of printing speed on FDM 3D-printed PLA samples produced using different two printers. International Journal of 3D Printing Technologies and Digital Industry, December 2022, Vol.6, No.3, pp 438-4. ISSN 2602-3350. https://doi.org/10.46519/ij3dptdi.1088805

[Kartal 2024] Kartal, F. & Kaptan, A. Response of PLA material to 3D printing speeds: A comprehensive examination on mechanical properties and production quality. European Mechanical Science, 2024, Vol.8, No.3, pp 137-144. ISSN 2587-1110. https://doi.org/10.26701/ems.1395362

[Kruzliak 2024] Kruzliak, J. Výskum degradácie pevnostných charakteristík výtlačkov pri vysokorýchlostnej 3D tlači (Research on the degradation of strength characteristics of printed parts for high-speed 3D printing). MTF-16687-11645. Trnava: Slovak University of Technology in Bratislava, Faculty of Materials Science and Technology, Institute of Production Technologies, 2024.

[Lorkowski 2025] Lorkowski, L., et al. Influence of Print Speed on the Mechanical Performance of 3D-Printed Bio-Polymer Polylactic Acid. Materials, April 2025, Vol.18, Article 1765. ISNN 1996-1944. https://doi.org/10.3390/ma18081765

[Miazio 2019] Miazio, Ł. Impact of print speed on strength of samples printed in FDM technology. Agricultural Engineering, 2019, Vol.23, No.2, pp 33-38. ISNN 2083-1587. https://doi.org/10.1515/agriceng-2019-0014

[Medellin-Castillo 2019] Medellin-Castillo, H.I. & Zaragoza-Siqueiros, J. Design and Manufacturing Strategies for Fused Deposition Modelling in Additive Manufacturing: A Review. Chinese Journal of Mechanical Engineering, 2019, Vol.32, No.1, pp 217-275. ISSN 2192-8258. https://doi.org/10.1186/s10033-019-0368-0

[Polymaker 2023a] PolyLite™ PLA [online]. [16.04.2025]. Available form <https:// polymaker.com/product/polylite-pla/>

[Polymaker 2023b] Polymaker Launches New High-Speed 3D Printing Filament - PolySonicTM PLA & PLA Pro [online]. [16.04.2025]. Available form <https://polymaker.com/polysonic-polymakers-new-family-of-high-speed-filament-showsthe-future-of-high-speed-3d-printing/>

[Redwood 2017] Redwood, B., Garrett, B. & Schöffer, F. The 3D printing handbook: technologies, design and applications. Amsterdam: 3D Hubs. ISBN 978-90-827485-0-5

[Siemiński 2021] Siemiński, P. 2021. In: Pou, J., Riveiro, A. and Davim. J.P., ed. Handbooks on Advanced Manufacturing, Additive Manufacturing. Chapter 7 - Introduction to fused deposition modeling. Elsevier, pp 217–275. ISBN 978-0-12-818411-0

[Tinius Olsen 2024] 300ST model of Electromechanical Universal Testers from Tinius Olsen [online]. [16.04.2025]. Available form <https://www.tiniusolsen.com/product/model-300st/>

CONTACTS:

doc. Ing. Ladislav Morovic, PhD.
Slovak University of Technology in Bratislava
Faculty of Materials Science and Technology in Trnava
Institute of Production Technologies
Ulica Jana Bottu 2781/25, 917 24 Trnava, Slovakia

+421 918 600 176, ladislav.morovic@stuba.sk, https://www.stuba.sk/ , https://www.mtf.stuba.sk/